Environmental Science: Atmospheres

ROYAL SOCIETY OF CHEMISTRY

PAPER

View Article Online
View Journal

Cite this: DOI: 10.1039/d6ea00013d

Multi-year submicron aerosol chemical composition at a high-altitude site in the Western Ghats of India

Sonal Kumari, * G. Pandithurai, Pallavi Padwal, Rohit D. Patil, V. Anil Kumar, P. P. Leena, Sachin S. Patil, Ajit Waware and Lalit R. Chaudhari

Organic aerosols (OAs) are the key factors influencing air quality and climate change. Studies providing long-term characterizations of the highly time-resolved chemical composition of aerosols and the sources of OAs in the ambient air remain limited due to the challenges associated with continuous observations. Here, we present an analysis of the long-term variability of submicron aerosols using an Aerosol Chemical Speciation Monitor (ACSM). The study presents the interannual and interseasonal measurements of non-refractory submicron particulate matter with aerodynamic diameter ≤1 μm (NR-PM_1) at a high-altitude site in the Western Ghats of India from October 2015 to February 2018. The mean NR-PM_1 concentration observed during the study period was 9.5 ± 8.5 μg m^{-3}, dominated by OAs (55 ± 16%) followed by sulphate (SO_4, 27 ± 13%), ammonium (NH_4, 11 ± 6%), nitrate (NO_3, 6 ± 4%), and chloride (Cl, 1 ± 0.5%). The percentage contribution of NR-PM_1 species across different years showed some disparity when compared by season. The diurnal pattern of OAs closely resembled that of NR-PM_1, while NH_4 exhibited a combined diurnal pattern of SO_4 and NO_3. Similar diurnal patterns of NR-PM_1 species were observed across years in each season, though with varying magnitudes. The highest seasonal average concentrations of NR-PM_1, OAs, NO_3 and NH_4 were observed during the winter season, followed by the post-monsoon season. Source apportionment of OAs was carried out using Positive Matrix Factorization (PMF). Secondary factors contributed markedly in the winter, post-monsoon, and summer seasons in 2015 and 2017, whereas in 2016, primary and secondary OAs contributed nearly equally.

Received 23rd January 2026
Accepted 24th April 2026

DOI: 10.1039/d6ea00013d

rsc.li/esatmospheres

Environmental significance

Understanding the long-term variability in aerosol composition and sources is essential for accurately assessing regional air quality, climate forcing, and atmospheric chemical processes, yet such datasets remain rare in South Asia. This multi-year, high-time-resolution characterization of submicron aerosols at a high-altitude site in the Western Ghats provides critical insight into seasonal and interannual controls on organic aerosol formation and secondary aerosol dominance. By capturing background and transported pollution influences in a climatically sensitive region, this work supports improved representation of aerosols in regional climate models and informs air quality mitigation strategies across the Indian subcontinent.

1 Introduction

Atmospheric particulate matter (PM) originates from natural and anthropogenic sources.[1] Primary aerosols are emitted directly from sources, whereas secondary aerosols are formed from gaseous precursors *via* atmospheric oxidation and subsequent partitioning into the aerosol phase.[2] The atmospheric fate and concentration of ambient PM depend on numerous factors, including primary emissions, meteorological conditions, and atmospheric oxidizing capacity.[3] Exposure to ultrafine particulate matter (PM_1) is a major risk factor for respiratory and cardiovascular diseases; fine particulate matter ($PM_{2.5}$) alone contributes to ~4.2 million premature deaths annually.[4] Given that PM_1 represents a significant fraction of $PM_{2.5}$ and can penetrate deeply into the alveolar region, it is likely to play a critical role in driving these health impacts.

Organic aerosols (OAs) constitute a major fraction of submicron particulate matter, typically contributing ~40–80% at regional and high-altitude sites, and play a critical role in climate and air quality.[5] The complexity of OAs arises from their highly variable composition and physicochemical properties, including oxidation state, volatility, viscosity, and hygroscopicity.[6–9] These properties directly influence atmospheric impacts; for example, highly oxidized and hygroscopic

Atmospheric Research Testbeds-High-Altitude Cloud Physics Laboratory (ART-HACPL), Indian Institute of Tropical Meteorology (IITM), Ministry of Earth Sciences, Pashan, Pune, 411008, India. E-mail: sonal.kumari@tropmet.res.in

OAs enhance cloud condensation nuclei (CCN) activity, increasing cloud droplet number concentration and radiative cooling, while low-volatility and viscous OAs can extend the atmospheric lifetime by reducing evaporation and chemical reactivity. Additionally, variations in the oxidation state of OA (*e.g.*, the O : C ratio) are closely linked to secondary organic aerosol (SOA) formation and aging processes, which govern aerosol optical properties and their contribution to radiative forcing.

To assess and identify the sources of OA emissions, aerosol mass spectrometry (AMS)[10] and aerosol chemical speciation monitor (ACSM)[11,12] are widely employed.[13–15] AMS provides high time resolution (seconds to minutes) and detailed size-resolved chemical composition, but its operation requires frequent calibration, high maintenance, and significant operational expertise, limiting its applicability for long-term continuous measurements.[16,17] In contrast, ACSM is designed for long-term monitoring with lower operational complexity, reduced maintenance requirements, and improved instrument stability, making it particularly suitable for extended deployments (>1 year). However, ACSM has certain limitations compared to AMS, including lower time resolution (typically 15–30 minutes), reduced sensitivity, and a lack of size-resolved measurements. The detection limits for ACSM are generally on the order of ~0.2–0.5 μg m^{-3} for major non-refractory species, and the uncertainties in the measured concentrations can range from ~20–30%, influenced by factors such as collection efficiency, ionization efficiency, and aerosol composition. Despite these limitations, ACSM provides reliable measurements of bulk non-refractory PM_1 composition and is well-suited for capturing long-term trends and seasonal variability. For high-altitude sites, where logistical constraints and the need for continuous, multi-year observations are critical, ACSM offers a practical and robust solution. Its ability to operate autonomously with minimal maintenance makes it particularly advantageous for remote environments, enabling the investigation of long-term aerosol evolution, source apportionment, and regional atmospheric processes.

At high-altitude sites, aerosols, depending on their size and composition, can be transported over long distances,[18–20] and undergo continuous aging during transport, leading to changes in their physical and chemical properties.[21,22] Aerosols at such locations play a crucial role in aerosol–cloud interactions by acting as cloud condensation nuclei (CCN) and ice nuclei (IN).[23] For instance, hygroscopic particles such as sulphate and highly oxidized organic aerosols can readily act as CCN, leading to the formation of cloud droplets with higher number concentrations but smaller sizes. This can enhance cloud reflectivity (the albedo effect) and prolong cloud lifetime by suppressing precipitation. Similarly, certain particles such as mineral dust and black carbon can act as ice nuclei, influencing the formation of ice crystals in mixed-phase clouds and thereby altering cloud structure and precipitation patterns. These processes can significantly impact regional radiation balance and hydrological cycles. For example, increased aerosol loading can lead to brighter and longer-lived clouds, which may reduce solar radiation reaching the surface (aerosol indirect effects). In addition, cloud processing can further modify aerosol properties through aqueous-phase reactions, leading to the formation of secondary species, such as sulphate and secondary organic aerosols (SOA), thereby influencing aerosol composition and hygroscopicity. Aerosols at high-altitude sites can also impact surface-level air quality through downward mixing of aged and processed particles.[24] Therefore, measurements at high-altitude regions are essential for understanding the complex interplay between aerosol properties, cloud microphysics, and their broader climatic and air quality implications.[25]

Despite the global prevalence of studies utilizing mass spectrometers, such observations remain scarce in India. This region boasts a diverse array of sources for aerosols and precursors, as highlighted in studies by Acharja *et al.*,[26] Ajith *et al.*,[27,28] Bhandari *et al.*,[29,30] Cash *et al.*,[31] Chakraborty *et al.*,[32] Dave *et al.*,[33] Gani *et al.*,[34] Gunthe *et al.*,[35] Kommula *et al.*,[36] Kompalli *et al.*,[37,38] Lalchandani *et al.*,[39] Mukherjee *et al.*,[40] Patel *et al.*,[41] Singh *et al.*,[42] Thamban *et al.*[43] and Vispute *et al.*[44] These studies have either focused on a single season, a single year, the impact of COVID-19, or a discontinuous multiyear comparison. The limited availability of long-term measurements hampers the understanding of the sources, formation, and evolution of OAs in India. This underscores the need for observations under diverse atmospheric conditions. To address this gap, the present study provides a multi-year investigation of non-refractory submicron particulate matter with aerodynamic diameter ≤1 μm (NR-PM_1) aerosols at a high-altitude site in the Western Ghats of India. High-altitude environments are often influenced by regionally transported and aged air masses, which are typically enriched in secondary organic aerosols (SOAs) formed through the oxidation of precursor gases during transport. As a result, such sites are expected to exhibit a higher contribution of oxygenated organic aerosols (OOAs), reflecting the dominance of secondary formation processes over primary emissions. In this context, the present study aims to address the following key research questions:

(i) What are the seasonal and interannual characteristics of NR-PM_1 and its chemical components at a high-altitude site?

(ii) What are the dominant sources of OA, and what is the relative contribution of primary *versus* secondary organic aerosols?

(iii) To what extent do meteorological parameters influence the formation and variability of NR-PM_1 species?

To answer these questions, we analyse diurnal, seasonal, and interannual variability of NR-PM_1 and its components and apply Positive Matrix Factorization (PMF) to apportion OA sources. This comprehensive analysis provides insights into the processes governing aerosol composition at a high-altitude regional background site and helps inform effective mitigation strategies.

2 Methodology

2.1. Sampling site

The measurements were conducted at the High-Altitude Cloud Physics Laboratory (HACPL) located in Mahabaleshwar (17.92 °N, 73.65 °E; 1378 m above mean sea level) during

Fig. 1 The location of the HACPL observation site situated at Mahabaleshwar (marked in red).

October 2015 – February 2018 (Fig. 1). The site is situated on the mountainous Sahyadri range of the Western Ghats along the western coast of India. Mahabaleshwar is a plateau (~150 km^2) surrounded by valleys, which influences local meteorology and air mass movement. Due to its high-altitude location and relatively low population density (~12 700), the site can be broadly considered representative of a regional background environment. However, local influences cannot be completely excluded, as nearby residential activities, tourism-related emissions, and occasional small-scale biomass burning may intermittently affect the site. The site's elevated position allows it to intercept air masses transported from surrounding regions, including urban and industrial areas such as Pune and Mumbai, particularly under favourable meteorological conditions. Thus, the observations reflect a combination of regional background aerosol characteristics modulated by long-range transport. This makes the site well-suited for investigating regional aerosol processes, seasonal variability, and the influence of transported pollution over the Western Ghats.[45]

The current study classifies seasons based on the prevailing circulation features, with the following classifications: summer (March to May), monsoon (June to September), post-monsoon (October to November) and winter (December to February). This classification aligns with a previous study conducted over the same site.[40]

2.2. Measurements and data analysis

2.2.1. Time of flight-aerosol chemical speciation monitor (ToF-ACSM). In the present study, measurements of non-refractory submicron particulate matter with aerodynamic diameter ≤1 μm (NR-PM_1) were carried out using Time of Flight-Aerosol Chemical Speciation Monitor (ToF-ACSM, Aerodyne Research Inc.) during October 2015-February 2018. Detailed descriptions of the ACSM instrument, its operation, and calibration procedures are provided in earlier reported studies.[13,40,46] Briefly, the ACSM instrument operates as follows: the aerodynamic lens in the ACSM instrument alternates between sampling particle-laden and particle-free air, directing the particle beam into the ACSM instrument. The focused particle beam passes through the first two chambers before entering the detection chamber, where the non-refractory fraction undergoes flash vaporization in a hot oven (tungsten at 600 °C). The non-refractory constituents of the particles then vaporize and are ionized by electron impact, with electrons emitted from a tungsten filament positioned perpendicularly to the particle beam in the vaporization region (using an electron kinetic energy of 70 eV). The ion optics guide and focus the ions into the Time-of-Flight analyzer, where they are extracted orthogonally and seperated based on their mass-to-charge ratio. The lens system achieves nearly 100% transmission for vacuum aerodynamic diameters between 150 and 450 nm.[47] The ACSM data were recorded at a time resolution of 30 min, and all subsequent analyses were performed using these time-averaged values. In the present study, a collection efficiency (CE) of 0.5 was applied to the ACSM data to correct measured mass concentrations for particle transmission and bounce effects at the vaporizer. This correction was applied uniformly across the entire dataset. The use of CE = 0.5 is consistent with several previous AMS/ACSM studies under ambient conditions, where it has been shown to be appropriate for mixed inorganic–organic aerosols.[14,40] The chosen CE value is further supported by the dominance of neutralized aerosols in the present study (ANR ≈ 1), which typically corresponds to moderate particle phase water content and reduced particle bounce effects.

Although the instrument manufacturer does not prescribe a fixed CE value, this assumption is widely adopted in long-term field measurements in the absence of composition-dependent calibration. It is acknowledged that CE can vary with aerosol composition, phase state, and relative humidity, and may change over time. This variability may introduce an uncertainty of ~20–30% in the reported mass concentrations.

2.2.2. Meteorology. Meteorological parameters were recorded at 1-minute intervals by an Automatic Weather Station (AWS) at the HACPL site. Temperature (T), solar radiation (SR), relative humidity (RH), wind speed (WS), and accumulated rainfall were recorded. Planetary boundary layer height (PBLH) was extracted from the Global Data Assimilation System (GDAS) National Oceanic and Atmospheric Administration (NOAA) Air Resources Laboratory (ARL) (0.5° × 0.5°) meteorological data at 3 h temporal resolution (https://www.ready.noaa.gov/). It is important to note that GDAS-derived PBLH may carry substantial uncertainty over regions with complex terrain, such as the present high-altitude site in the Western Ghats. Therefore, the estimated PBLH values are treated as a first-order approximation of atmospheric mixing conditions. They are useful for identifying broad seasonal and diurnal trends; however, small differences should be interpreted with caution and not overemphasized. 3-Day backward air mass trajectories (seasonally grouped for the October 2015-February 2018 period) arriving at 500 m above the ground level (agl) were computed using the NOAA HYSPLIT (HYbrid Single Particle Lagrangian Integrated Trajectory) Model.

2.2.3. Positive matrix factorization (PMF). Positive matrix factorization (PMF) is a statistical model pioneered by Paatero and Tapper[48] that employs the least-squares method and incorporates non-negativity constraints on factors. It is widely adopted in the aerosol community for source-apportionment analysis.[49–51] In PMF analysis, the data matrix is represented as a linear combination of different factors with constant mass spectra and varying concentrations across the dataset.[52] For the seasonally grouped datasets (summer, monsoon, post-monsoon, and winter), the Unit Mass Resolution (UMR) matrix (m/z 12–220) and error matrix were generated using Tofware software (written in Igor Pro Wave metrics, Inc. Oregon USA) following the protocol outlined in Ulbrich *et al.*[53] Ions with m/z up to 120 were selected for PMF analysis due to their lower signal-to-noise ratio (S/N) as compared to larger m/z (>120) ions. Ions with 0.2 < S/N < 2 were down-weighted by a factor of 2, whereas ions with S/N ratios less than 0.2 were removed. To avoid additional weighting of CO_2^+, the errors of related ions (*e.g.*, O^+, HO^+, H_2O^+, and CO^+) were also down-weighted. Rotational ambiguity was tested by varying the forcing parameter, F_{peak}, between −1 and 1 in increments of 0.2, and PMF solutions were examined for up to 7 factors (Fig. S1).

3 Results and discussion

3.1. Temporal variation of NR-PM_1

Fig. 2 shows the temporal variation of the chemical components of NR-PM_1 at the study site from October 2015 to February 2018. The mean concentration of NR-PM_1 for the study period was 9.5 ± 8.5 μg m^{-3}. OA was the most abundant chemical component with 55 ± 16% contribution to NR-PM_1, followed by sulphate (SO_4, 27 ± 13%), ammonium (NH_4, 11 ± 6%), nitrate (NO_3, 6 ± 4%) and chloride (Cl, 1 ± 0.5%). A similar trend of NR-PM_1 chemical composition has been reported by other studies.[28,31,35,36] Monthly means of NR-PM_1 ranged from 1.6 to 20 μg m^{-3}. The organic aerosol with the most abundant fraction in NR-PM_1 showed monthly mean values varying from 1 to 11.8 μg m^{-3}, exhibiting higher concentration in winter months. The aerosol neutralization ratio (ANR) was evaluated using the ratio of ACSM measured NH_4^+ ($NH_4^+{}_{meas}$) to the predicted NH_4^+ ($NH_4^+{}_{pred} = 18 \times (2 \times SO_4/96 + NO_3/62 + Cl/35.5)$) required to fully neutralize sulphate, nitrate, and chloride.[54] The $NH_4^+{}_{meas}$ strongly correlated with $NH_4^+{}_{pred}$ ($r^2 = 0.9$), yielding a regression slope of 0.8. The average ANR during the study period was

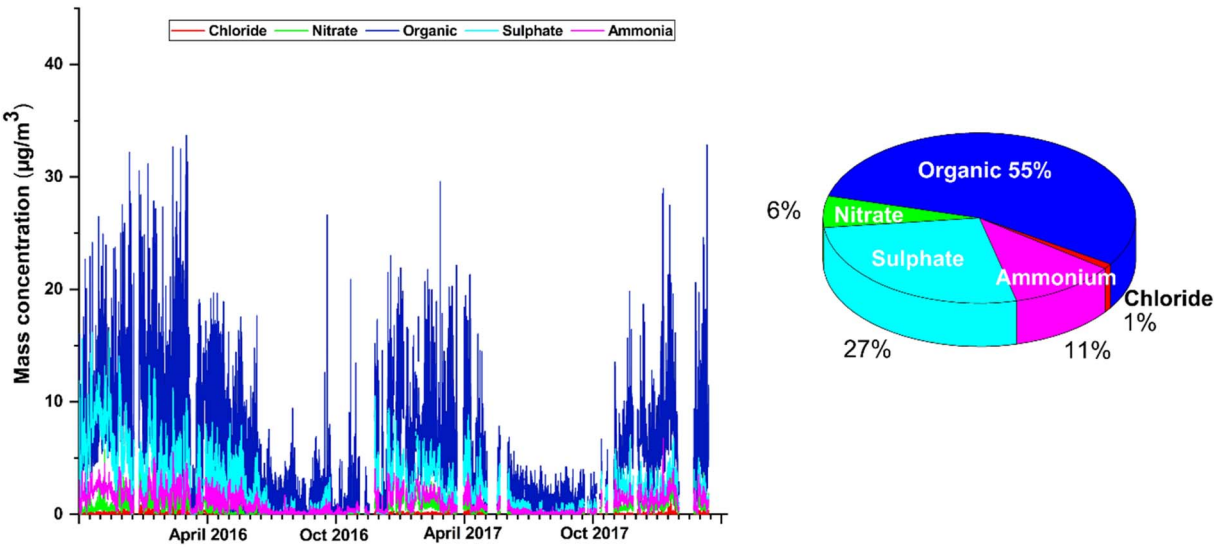

Fig. 2 Temporal variation of NR-PM_1 species and percentage contribution from October 2015 to February 2018.

1.2 ± 1.0. The results suggest that aerosol particles during the study period were neutralized. This may be attributed to enhanced conversion of NH_3 to NH_4^+ at low temperatures and high relative humidity.[1] Similar neutral aerosol particles were also reported at an urban site in India.[55] The predominance of neutralized aerosols has important implications for aerosol acidity and chemical processing. Near-neutral conditions favour the partitioning of semi-volatile inorganic species such as nitrate into the particle phase, thereby enhancing secondary inorganic aerosol formation. In addition, reduced aerosol acidity can influence heterogeneous chemistry by altering reaction rates and pathways on particle surfaces. From an organic aerosol perspective, near-neutral conditions facilitate aqueous-phase processing within particle liquid water, which can promote the formation of a secondary organic aerosol (SOA) through pathways such as the oxidation of water-soluble organic precursors. These conditions are particularly conducive to the formation of more oxidized and low-volatility organic species, contributing to the observed dominance of oxygenated organic aerosols (OOAs). Therefore, the neutralized nature of aerosols reflects efficient ammonia buffering and plays a critical role in governing both inorganic and organic secondary aerosol formation pathways.

3.1.1. Seasonal variation. The highest concentration of NR-PM_1 was observed during the winter season (14 ± 9 μg m^{-3}), followed by the post-monsoon season (11.8 ± 9 μg m^{-3}), summer season (8.9 ± 7.9 μg m^{-3}), and monsoon season (2.3 ± 2.1 μg m^{-3}), averaged over October 2015 to February 2018. The year-to-year seasonal variation followed the same trend. The elevated concentrations observed during the winter season can be attributed to increased biomass burning for heating (supported by the presence of BBOA factor identified through PMF analysis Section 3.3), along with meteorological conditions such as lower temperatures, higher relative humidity, and reduced wind speeds (Tables 1 and S1). These conditions lead to a shallow planetary boundary layer and frequent temperature inversions, which suppress vertical mixing and limit pollutant dispersion, thereby promoting the accumulation of pollutants near the surface.[1] The lowest concentration during the monsoon season is attributed to the wet scavenging of aerosols by rainfall.[56] Relatively higher concentrations were observed in the summer season compared to the monsoon season, which may be due to increased photochemical activity at higher temperatures and lower relative humidity, contributing to the enhanced formation of secondary organic aerosols (SOA).[57] Higher emission of biogenic VOCs from local vegetation also contributes to SOA formation.[58] However, in summer 2016 (12.2 ± 7.6 μg m^{-3}), concentrations were higher than in the post-monsoon season (3.6 ± 2.5 μg m^{-3}), which may reflect the combined influence of meteorological variability, including reduced rainfall (73% less) and differences in atmospheric mixing height (Table 1).

The seasonal average NR-PM_1 mass loading over Mahabaleshwar is comparatively lower than that observed in other regions of India. For instance, megacity New Delhi exhibits significantly higher NR-PM_1 mass loadings (*e.g.*, 195 μg m^{-3} in winter), which can be attributed to the dense population, intense vehicular emissions, industrial activities, and regional pollution transport.[34] Similarly, Kanpur, an urban-industrial centre located in the Indo-Gangetic Plain, reports elevated concentrations due to high emission density and unfavourable dispersion conditions.[55] In contrast, the relatively lower NR-PM_1 levels observed at Mahabaleshwar can be linked to its high-altitude location and comparatively lower local emission sources, which promote better dispersion and reduced pollutant accumulation. A coastal site such as Bhubaneswar shows comparable concentrations, likely due to the combined effects of moderate emissions and enhanced atmospheric mixing influenced by marine air masses.[37] Similarly, observations from Thumba indicate higher concentrations than the present study, reflecting differences in local emission sources and coastal atmospheric dynamics.[28]

The study period averaged seasonal trends of organics, nitrate and ammonium were similar to NR-PM_1. Conversely, sulphate showed the highest concentration in the post-monsoon season (4 ± 3.7 μg m^{-3}), followed by winter (3.3 ± 2.4 μg m^{-3}), summer (2.5 ± 1.8 μg m^{-3}) and the monsoon season (0.4 ± 0.9 μg m^{-3}). This seasonal pattern represents the average over all study years; however, some interannual variability was observed, with relatively higher sulphate concentrations during the post-monsoon season in a specific year (2015), influencing the overall mean. Chloride showed similar

Table 1 Seasonal average solar radiation (SR), relative humidity (RH), temperature (*T*), planetary boundary layer height (PBLH), wind speed (WS) and accumulated rainfall at the study site during October-2015-Feburary 2018

		SR (W m^{-2})	RH (%)	*T* (°)	PBLH (m)	WS (m s^{-1})	Accumulated rainfall (mm)
POSTMONSOON	2015	235.8 ± 301.2	59.9 ± 14.3	25.8 ± 3.7	378.9 ± 612.4	2.3 ± 1.2	237.1
	2016	230.8 ± 298.4	60.1 ± 18.2	23.2 ± 4.3	292.1 ± 493.7	2.1 ± 1.1	174.1
	2017	232.6 ± 300.8	58.9 ± 15.3	24.4 ± 3.6	377.7 ± 581	2.2 ± 1.2	190.6
WINTER	2015	227.4 ± 301.1	46.5 ± 15.1	23.8 ± 5.1	388.6 ± 616.1	2.4 ± 1.3	0
	2016	227.8 ± 305.1	46.4 ± 17	22.3 ± 5.6	384 ± 636.5	2.2 ± 1.3	0
	2017	222.1 ± 298.3	44.9 ± 16	22.5 ± 3.9	441.9 ± 718.7	2.1 ± 1.3	7.7
SUMMER	2016	286.8 ± 352.3	44.8 ± 21.8	28.8 ± 4.6	821.5 ± 1003	2.9 ± 1.4	39
	2017	289.1 ± 356.5	40.9 ± 23	28.2 ± 5.5	880.7 ± 1148.8	2.9 ± 1.3	146.5
MONSOON	2016	215.6 ± 291.5	82.4 ± 11.9	24.2 ± 3	612.6 ± 327.6	3.7 ± 1.8	6664.7
	2017	219.1 ± 296.9	78 ± 11.5	24.2 ± 2.7	712.7 ± 374.6	4.1 ± 1.9	5527.9

concentrations in the post-monsoon, summer and monsoon seasons (0.1 μg m^{-3}); however, the percentage contribution of Cl to NR-PM_1 was higher (4%) in the monsoon season than in other seasons. Over the entire season, the organics contribution to NR-PM_1 mass concentration was maximum (45–71%), followed by sulphate (14–40%), ammonium (8–14%), nitrate (3–9%) and chloride (0.4–4%) (Fig. 3). The highest contribution of OA during the monsoon season was observed when the air masses at the study site arrived from the Arabian sea (further discussed in Section 3.2). A study by Kommula *et al.*[36] from an urban coastal site in Chennai, India, also reported a higher contribution of OA (>60%), particularly during periods characterized by a clean marine air mass. During the winter and summer seasons, the OA contribution to NR-PM_1 composition was similar across different years. However, during the post-monsoon season, the OA contribution in 2015 was comparatively lower than that in 2016 and 2017. However, the SO_4 contribution increased from 20–24% to 40% in 2015. The elevated sulphate levels in 2015, despite relatively higher rainfall (237 mm), suggest a complex balance between removal and formation processes. While wet scavenging typically reduces aerosol concentrations, sulphate can be efficiently produced *via* aqueous-phase oxidation of SO_2 within cloud droplets under high relative humidity conditions (~60%). This in-cloud processing can enhance sulphate mass and partially offset its removal by precipitation. In addition, trajectory analysis indicates that during the post-monsoon season, ~95% of air masses originated from the continental region in 2015, reflecting a transition from marine to land-influenced air masses (Section 3.2). Such continental air masses are likely enriched in SO_2 and other precursor gases from anthropogenic sources, which can enhance secondary sulphate formation during transport and cloud processing. Therefore, the higher sulphate contribution observed in 2015 is likely driven by the combined effects of (i) enhanced aqueous-phase production under humid conditions, (ii) transport of precursor-rich continental air masses, and (iii) variable scavenging efficiency, rather than wet removal alone. The NO_3 concentration in 2015 was also comparatively lower (4%) than in 2016 (8%) and 2017 (7%). The reason for this disparity in 2015 could be due to the dominance of secondary aerosol formation favouring higher NO_3 and SO_4 levels.[59]

After OA, sulphate emerges as the second most dominant species across all seasons in this study. The highest contribution of SO_4 is observed during the post-monsoon season at 20–40%, with moderate contributions of 20–25% and 28% during winter and summer and the lowest (14–19%) during the monsoon season. The year-to-year contribution of SO_4 showed variation; for example, in the post-monsoon season of 2015, SO_4 exhibited the highest contribution (40%), which was comparatively higher than in the 2016 and 2017 seasons. During the winter season, the SO_4 contribution in 2015 and 2016 was similar, but higher than in 2017. Both years in the summer season showed a similar SO_4 contribution, while the monsoon season showed a different contribution. Ammonium, nitrate and chloride also exhibit seasonal variabilities, although with less variation compared to organics. Nitrate, serving as an indicator of anthropogenic emissions, remains consistent throughout the year with a mass fraction of approximately 3–9%, indicative of less-polluted air masses prevailing over Mahabaleshwar compared to other urban regions of India.

3.1.2. Diurnal variation. Fig. 4 shows the diurnal variability of NR-PM_1 and its species across different seasons and years. The comparison reveals distinct temporal patterns, likely governed by a combination of emission timing, boundary layer

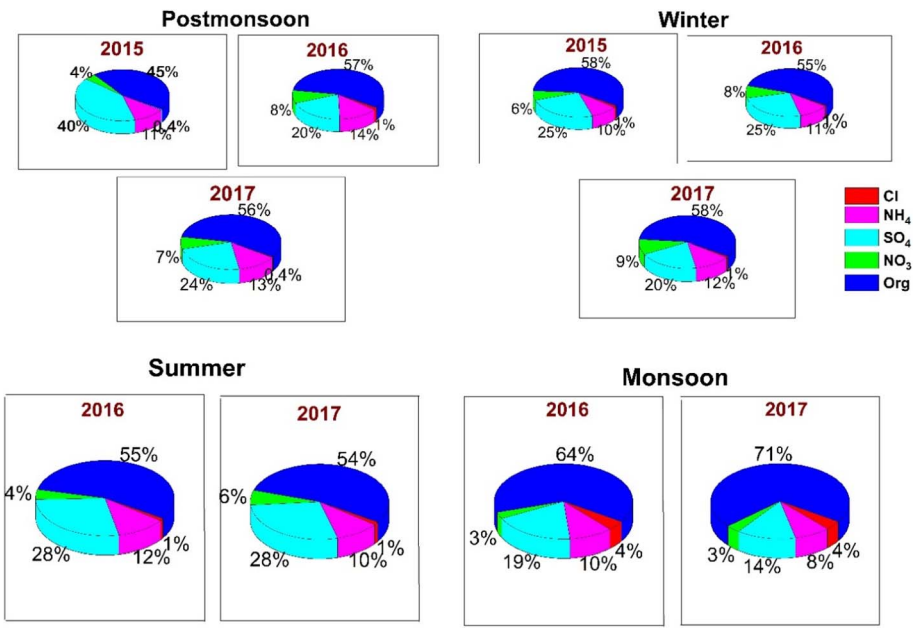

Fig. 3 Percentage contribution of NR-PM_1 species during the post-monsoon, winter, summer and monsoon seasons during Oct 2015-Feb 2018.

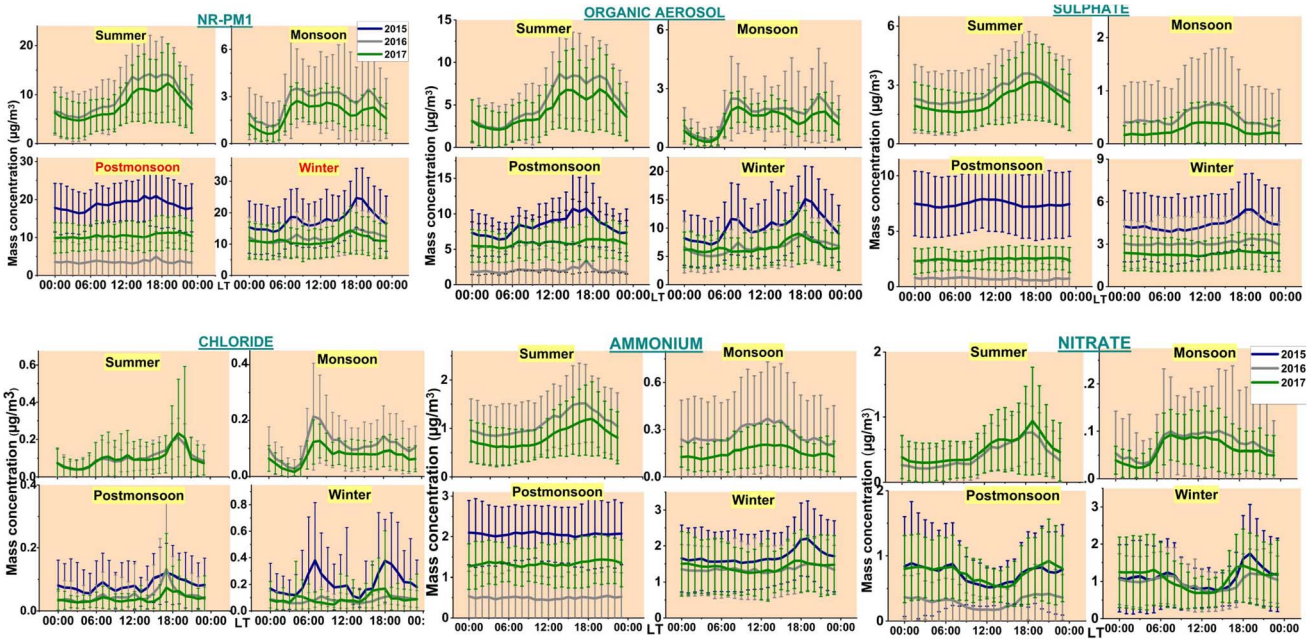

Fig. 4 Seasonal diurnal plots of NR-PM_1 and its species over the study period.

dynamics, and atmospheric processing. During summer, NR-PM_1 exhibited a gradual increase starting at noon, and reaching a maximum in the evening, followed by a decline to early morning minima. In winter, a bimodal pattern was observed, with peaks in the early morning and late night, whereas the post-monsoon season showed relatively weak diurnal variability. Interannual comparison indicates that diurnal patterns were broadly consistent in 2016 and 2017, with comparatively higher values observed in 2015 during the post-monsoon season. Organic aerosols exhibited diurnal trends similar to NR-PM_1. In summer, a pronounced midday build-up was observed, while in the monsoon and winter seasons, both morning and evening enhancements were evident along with a midday increase. The post-monsoon season showed a relatively flat diurnal profile, except in 2015. The observed morning and evening enhancements in organic aerosols are consistent with typical emission patterns associated with human activities and reduced boundary layer height during these periods, which can favour pollutant accumulation. The midday increase, particularly in summer, coincides with periods of enhanced solar radiation and atmospheric mixing, suggesting the possible influence of photochemical processing and secondary aerosol formation.[60] The yearly averaged diurnal values showed comparable concentration in 2016 and 2017. A Similar diurnal variation of OA has been observed by Vispute *et al.*[44] at a nearby urban site in Pune.

Sulphate exhibited moderate diurnal variability, governed by both gas-phase and aqueous-phase formation pathways. The daytime increase in sulphate concentrations during the summer, monsoon, and post-monsoon seasons suggests the dominance of gas-phase oxidation of SO_2 by OH radicals, leading to the formation of H_2SO_4 and subsequent partitioning into the particle phase. This process is enhanced under high solar radiation and oxidant availability.[61] In contrast, during winter, the negligible daytime enhancement and the pronounced evening peak indicate the increased importance of aqueous-phase oxidation pathways. Under conditions of high relative humidity and reduced planetary boundary layer (PBL) height, dissolved SO_2 (as S(IV)) is oxidized in particle liquid water by oxidants such as H_2O_2 and O_3, leading to efficient sulphate production. These processes are further facilitated by stagnant conditions that enhance precursor accumulation and aerosol liquid water content. The sharp decline in sulphate concentration during the post-monsoon season in 2016 (from 7.5 µg m^{-3} in 2015 to 0.7 µg m^{-3} in 2016) suggests substantial interannual variability in precursor availability and/or atmospheric oxidation capacity, influencing secondary aerosol formation pathways. In contrast, consistently low sulphate levels during the monsoon season (as low as 0.2 µg m^{-3} in 2017) highlight the dominant role of wet scavenging, which efficiently removes both precursors and formed sulphate from the atmosphere. Overall, these observations indicate that gas-phase oxidation dominates sulphate formation during periods of high photochemical activity, whereas aqueous-phase processes become significant under high RH and stagnant wintertime conditions. Nitrate exhibited distinct diurnal patterns across seasons. In summer, a daytime build-up was observed, which may be associated with enhanced photochemical production and local emissions. In contrast, during the post-monsoon and winter seasons, a bimodal diurnal pattern with lower daytime and higher nighttime concentrations was evident. The pronounced wintertime enhancement in nitrate is consistent with temperature-dependent gas–particle partitioning of semi-volatile ammonium nitrate (NH_4NO_3).[62] At lower temperatures, the equilibrium shifts toward the particle phase, favouring the formation and stabilization of particulate nitrate,

whereas higher daytime temperatures promote its volatilization back to the gas phase (as NH_3 and HNO_3). Additionally, reduced boundary layer height and weaker dispersion during nighttime can further enhance near-surface accumulation. Therefore, the observed winter dominance of nitrate is likely influenced by a combination of thermodynamic partitioning and meteorological conditions. However, nitrate was consistently low during the monsoon season, where the concentrations fell to 0.06–0.09 μg m^{-3}. Nitrate concentrations in 2015, 2016 and 2017 showed similar diurnal values, except during the post-monsoon season. Ammonium showed the combined diurnal pattern of sulphate and nitrate indicating the existence of NH_4 as $(NH_4)_2SO_4$ and NH_4NO_3.[63] Chloride, although a minor contributor, showed a notable variable diurnal pattern. Chloride showed two peaks of similar magnitude during early morning and evening in the winter season, whereas in other seasons, two peaks of different magnitude were observed. This suggests contributions from local sources like biomass burning and vehicles.[49] The highest Cl levels were observed in 2015. This comparative analysis of NR-PM_1 and its species demonstrates that organic aerosols and sulphate contribute significantly to the seasonal and interannual dynamics of NR-PM_1, with chloride, nitrate and ammonium showing subtler but consistent seasonal trends.[64]

3.2. Variation of the meteorological parameters

Meteorological parameters recorded by an Automatic Weather Station (AWS) at the HACPL site revealed maximum temperature (28.2–28.8 °C), intermediate relative humidity (40.9–44.8%), lower wind speed (2.9 m s^{-1}), and lower rainfall (39–146.5 mm) during the summer season (Table 1 and Fig. S2). The highest relative humidity (78–82.4%) and rainfall (5527.9–6664.7 mm) were observed in the monsoon season. The post-monsoon season showed increased temperature (23.2–25.8 °C), and reduced relative humidity (58.9–60.1%) and rainfall (174.1–237.1 mm) compared to the monsoon season. Relative humidity (44.9–46.5%), temperature (22.3–23.8 °C), wind speed (2.1–2.4 m s^{-1}) and rainfall (0–7.7 mm) in the winter season were lower compared to the post-monsoon season. Similar seasonal variation of the meteorological parameters has been reported by Gani *et al.*[34] On comparing inter-annual variation in each season, solar radiation showed minimal variation across years, suggesting similar solar radiation in different years in each season. Relative humidity showed slight interannual variability, particularly during the summer (44.8% in 2016 and 40.9% in 2017) and monsoon seasons (82% and 78% in 2016 and 2017, respectively). RH plays a critical role in modulating aerosol chemistry by influencing both heterogeneous reactions and hygroscopic growth processes. Elevated RH enhances the liquid water content of particles, facilitating aqueous-phase reactions that promote the formation of secondary inorganic aerosols such as sulphate and nitrate through the oxidation of SO_2 and NO_x. Additionally, increased RH supports the partitioning of semi-volatile species into the particle phase, thereby enhancing secondary organic aerosol formation. Hygroscopic growth under high RH conditions leads to an increase in particle size and alters the optical properties, which can further impact atmospheric radiative forcing and visibility. Moreover, the presence of particle-bound water accelerates heterogeneous reactions on aerosol surfaces, contributing to aging and increased oxygenation of organic aerosols. In contrast, lower RH conditions limit aqueous-phase processing and favour the presence of relatively fresher, less oxidized aerosols. Therefore, even modest seasonal and interannual variations in RH can significantly influence PM_1 composition, chemical transformation pathways, and atmospheric lifetime.[49] Temperature showed minimal interannual variability. Wind speed also remained consistent across all the years. During the monsoon season, the wind speed was slightly higher in 2017 (4.1 m s^{-1}) compared to 2016 (3.7 m s^{-1}), suggesting stronger winds in 2017. Accumulated rainfall showed notable differences between years, especially in the summer, monsoon and post-monsoon seasons. In summer, rainfall was higher in 2017 (146.5 mm) as compared to 2016 (39 mm). The monsoon season saw a decrease in rainfall from 6664.7 mm in 2016 to 5527.9 mm in 2017, reflecting variability in both the intensity and distribution of the monsoon rains. During the post-monsoon season, the lowest rainfall was observed in 2016. PBLH showed varied values across different years. In 2017, the highest PBLH was observed across all seasons. These results indicate that solar radiation, relative humidity, temperature and wind speed were comparable in all the years, whereas PBLH and accumulated rainfall showed variation across years.

To better understand the observed seasonal and interannual variability in aerosol composition, three-day backward air mass trajectories were clustered and analysed in conjunction with their associated chemical signatures (Fig. 5). The results highlight a strong dependence of aerosol composition on air-mass origin, with distinct differences between marine and continental influences. During the monsoon season, air masses were predominantly of marine origin (100% from the Arabian Sea), which corresponded to the lowest NR-PM_1 concentrations and reduced contributions from secondary inorganic aerosols (*e.g.*, sulphate and nitrate). This is consistent with enhanced wet scavenging and the relatively cleaner marine environment. In contrast, the post-monsoon season showed a clear transition to continental air masses, with ~78–95% of trajectories originating from inland regions. These air masses are likely enriched in anthropogenic precursors such as SO_2 and NO_x, which promote secondary aerosol formation. Notably, the post-monsoon season of 2015 exhibited a higher contribution of sulphate (~40%), which can be attributed to the combined influence of continental transport and enhanced aqueous-phase formation under relatively humid conditions. During the winter season, the dominance of north-westerly and north-easterly continental air masses further supports the influence of long-range transport from polluted regions. These air masses are associated with increased concentrations of organics and nitrate, reflecting contributions from combustion-related emissions and favourable conditions for gas-to-particle partitioning. In the summer season, the increased influence of marine air masses (63–71%) resulted in comparatively lower aerosol loading than in winter, although secondary organic aerosol formation remained significant due to enhanced photochemical activity.

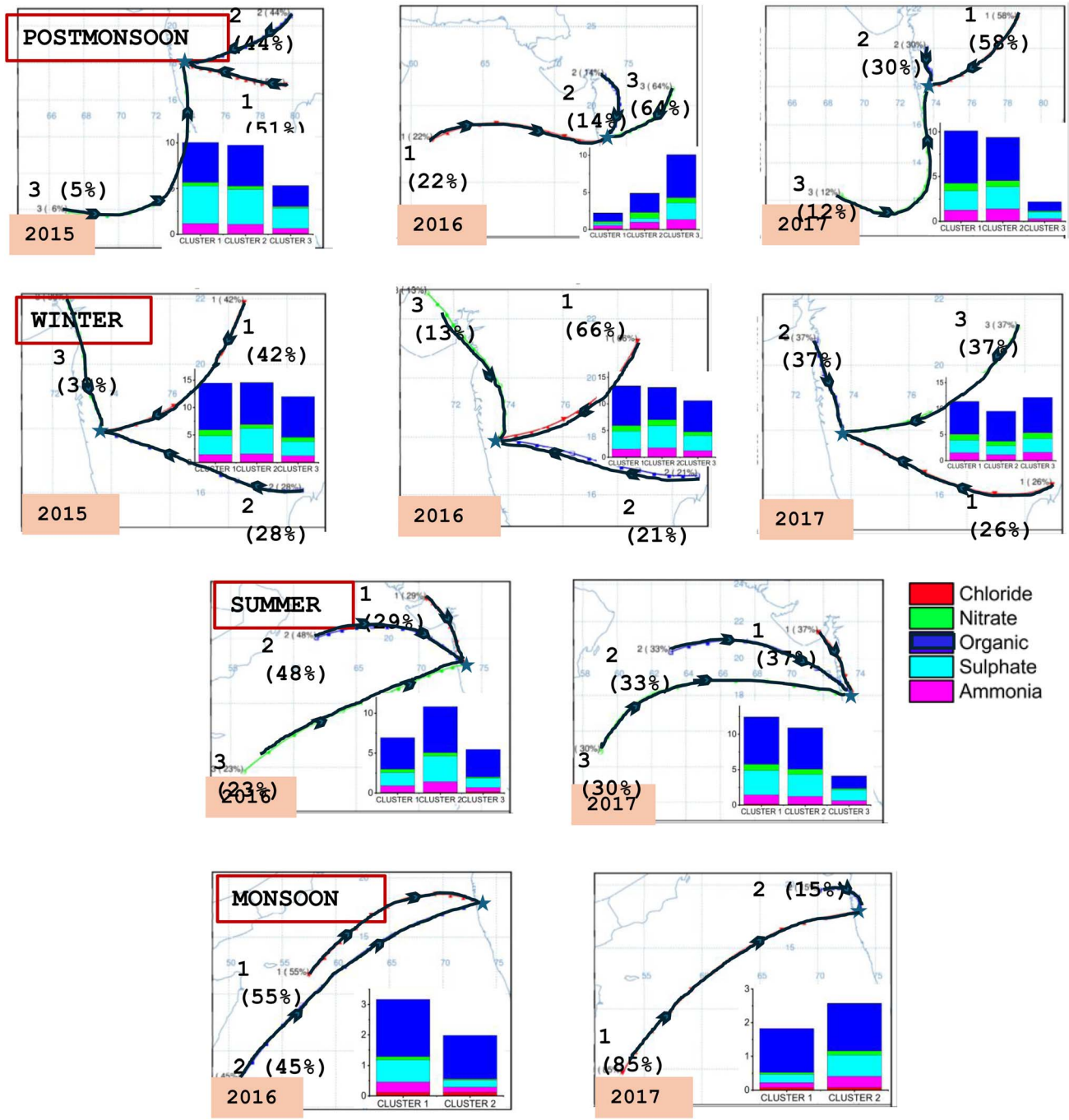

Fig. 5 Clusters of three-day backward air mass trajectories arriving at 500 m agl at the study site Mahabaleshwar (marked with a blue star) for the post-monsoon, winter, summer and monsoon seasons during October 2015–February 2018.

Importantly, interannual variability in aerosol composition is closely linked to changes in air-mass origin. For instance, variations in the relative contribution of continental *versus* marine trajectories across years explain differences in sulphate and organic aerosol fractions, particularly during the post-monsoon and summer seasons. These findings demonstrate that air-mass origin is a key controlling factor governing both the magnitude and composition of aerosols at this high-altitude site.

3.3. Source apportionment of OAs

In comprehending the characteristics of OAs throughout all seasons, it is crucial to delve into their specific attributes, particularly the nature of the sources and potential atmospheric evolution. To unravel the distinct OA factors originating from various sources, PMF analysis was conducted on the OA mass spectrum acquired through ACSM measurements. This analysis was performed separately for each season and year. A 4-factor solution was derived for the summer, post-monsoon and winter

seasons, while 3-factors were derived for the monsoon season following the criteria reported in a previous study by Mukherjee *et al.*[40] at the present study site (Fig. 6). The identified factors were validated by comparing them with mass spectra documented in the literature and accessible in the CV-based ACSM PMF mass spectrum database (https://cires1.colorado.edu/jimenez-group/AMSsd_CV/).

HOAs (Hydrocarbon-like Organic Aerosols), BBOAs (Biomass Burning Organic Aerosols) and OOAs (Oxygenated Organic Aerosols) are the factors obtained in this study. HOAs and BBOAs serve as effective proxies for primary OAs (POAs), while OOA-1 and OOA-2 are reliable surrogates for secondary OAs (SOAs). The HOA profile is characterized by peaks of aliphatic hydrocarbons (C_xH_y family) at masses *m*/*z* 27, 41, 43, 55, 57, 69, and 71.[65,66] In contrast, the BBOA profile is identified by a prominent signal of ions at *m*/*z* 29, 60, and 73, associated with the fragmentation of anhydrous sugars such as levoglucosan and mannosan.[67] The OOA is characterized by dominant ions at *m*/*z* 43 and *m*/*z* 44, contributed by $C_2H_3O^+$ and CO_2^+, respectively. These species play a crucial role in characterizing the formation of secondary aerosols. Additionally, tracer ions (*m*/*z* 43, 44, 60) for each source type exhibit strong correlations with the respective resolved factors, such as HOA, BBOA, and OOA (*e.g.*, a correlation coefficient of *m*/*z* 43 with HOA ~0.85).

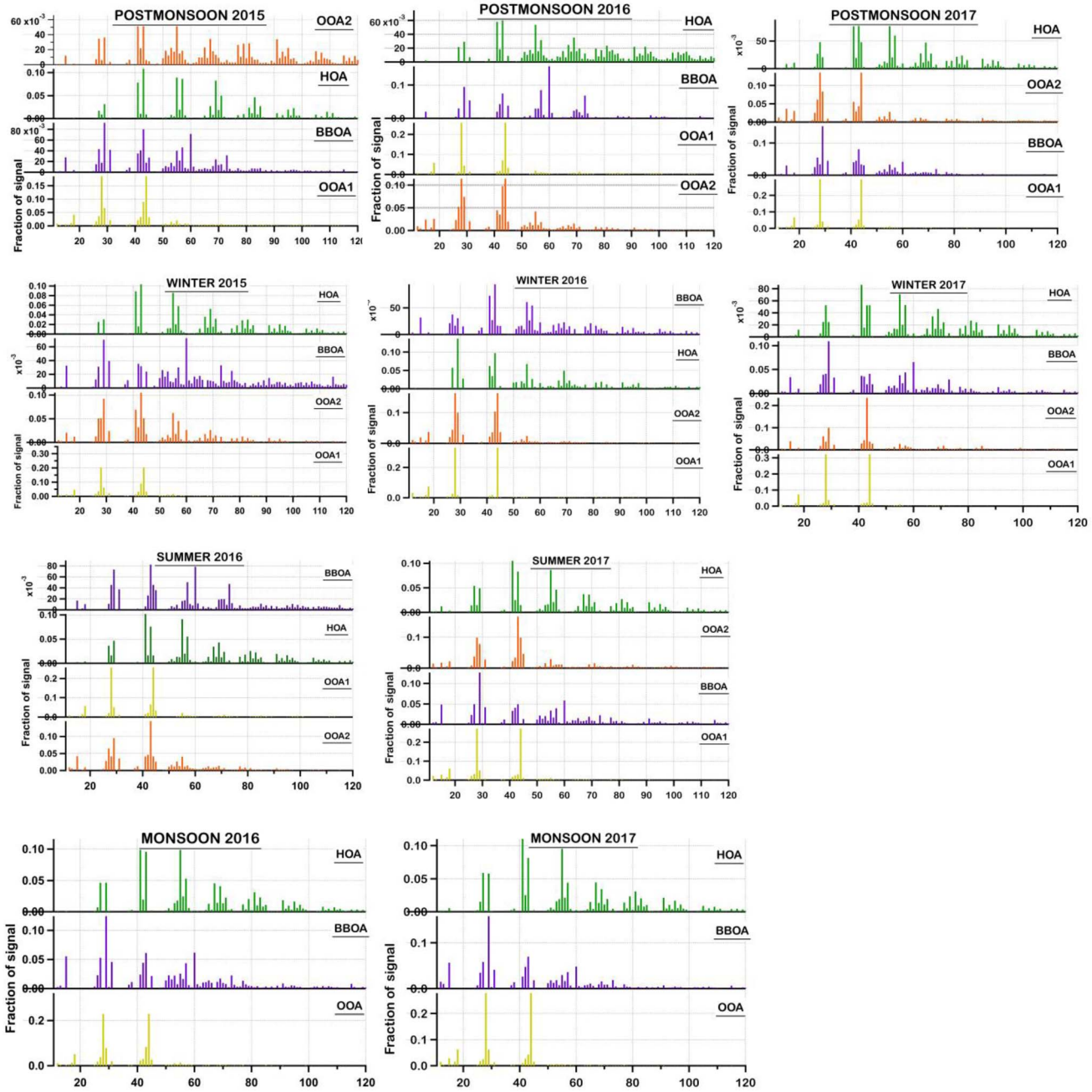

Fig. 6 Positive matrix factorization of organic mass spectra for the post-monsoon, winter, summer and monsoon seasons during 2015–2017.

In the post-monsoon season, the contribution of SOAs (OOA1-27–59% and OOA2-14–38%) was dominant over the primary OAs (HOA-12–25% and BBOA-8-13%) (Fig. 7). The OOA1 spectrum revealed significant contributions from oxygen-containing ions at m/z 44, along with a higher O : C ratio (1.2–1.4), thus characterizing it as an LV-OOA (low volatile OOA). In contrast, the OOA2 spectrum was characterized by non-oxygen-containing ions at m/z 29, 43, and 55, which dominated and displayed a lower O : C ratio (0.3–0.5), and was therefore identified as an SV-OOA (semi-volatile OOA). The consistent diurnal pattern observed in OOA1 and OOA2 suggests long-range transport of aerosols, characterized by well-mixed and more oxidized properties. OOA2 and SO_4 showed a good correlation (r^2 = 0.7) indicating similar sources. On comparing inter-annually, the OOA1 percentage contribution in 2016 showed relatively lower contribution to OA (27%) as compared to 2015 (55%) and 2017 (59%). On the other hand, the contribution of OOA2 increased in 2016 (38%) compared to 2015 (14%) and 2017 (17%). This discrepancy indicates the dominance of freshly formed SOAs from local emission in 2016. The diurnal variation of BBOAs showed peaks in the early morning and evening, attributed to biomass burning activities. On the other hand, HOAs showed a peak during evening hours due to the contribution from local vehicular emissions. The year-to-year trend showed the highest values in 2015. HOA showed the largest difference between 2015 and the years 2016–2017, indicating a stronger influence of vehicular emissions during 2015. The OOA1 diurnal values in 2016 were comparatively lower.

During the winter season, SOAs showed dominance in 2015 and 2017 with OOA1 ranging between 42–54% and OOA2 between 16–22%. Similar to the post-monsoon season, the OOA1 contribution to OA showed dominance over OOA2. Based on m/z 43 : 44 and O : C ratio, OOA1 and OOA2 are classified as an LV-OOA and SV-OOA. In 2016, the contribution from all OA factors was comparable (around 25%), indicating a similar contribution from both primary and secondary sources. This can be attributed to stable meteorological conditions, such as temperature inversion and stagnant air masses, along with the dominance of transported SOAs. The diurnal pattern of OOA2 in the winter season was different from that in the post-monsoon season. It showed a stable diurnal pattern in 2017; however, in 2015, a bimodal pattern with early morning and late-night peaks was observed. The peaks can be attributed to freshly formed SOA from local emission. In 2016, higher diurnal values of OOA2 were observed. Similar to OOA2, OOA1 also showed stable diurnal patterns in 2016 and 2017, whereas in 2015, a peak was observed during the early morning. A stable diurnal pattern of OOA1 suggested aged, highly oxidised, and transported aerosol particles. The contribution of BBOAs and HOAs to the OA varied between 12% to 29%, and 16% to 24%, respectively. The higher ratio of m/z 55 : 57 (1.4–1.7) suggested contributions from cooking emissions to the HOAs. HOAs showed a diurnal pattern with concentrations increasing throughout the day and reaching a maximum in the evening. Higher concentration at nighttime can be attributed to the trapping of vehicular emissions in the lower boundary layer. In 2016 and 2017, similar diurnal patterns were observed. BBOA also showed a similar diurnal pattern in all years with morning and night peaks. These two peaks can be attributed by residential burning activities.

During the summer season in 2016, the contributions from SOAs (51%) and POAs (49%) were similar, whereas in 2017, SOAs showed a higher contribution (65%) compared to POAs (35%). The OOA1 factor exhibited a significant level of oxygenation, primarily attributed to a heightened contribution from m/z 44 (0.25–0.28) and an elevated O : C ratio (approximately 1.2–1.3), whereas OOA2 showed lower oxygenation at m/z 44 (0.004–0.006) and O : C ratio (0.1–0.3), indicating local origin. The diurnal pattern of OOAs showed a gradual build-up during the daytime, suggesting secondary organic aerosol formation in high sunlight and temperature conditions. A similar diurnal pattern is reported by Mohr *et al.*[68] and Xu *et al.*[49] Along with a daytime peak, high values during the evening were also observed, which may be attributed to enhanced condensation of

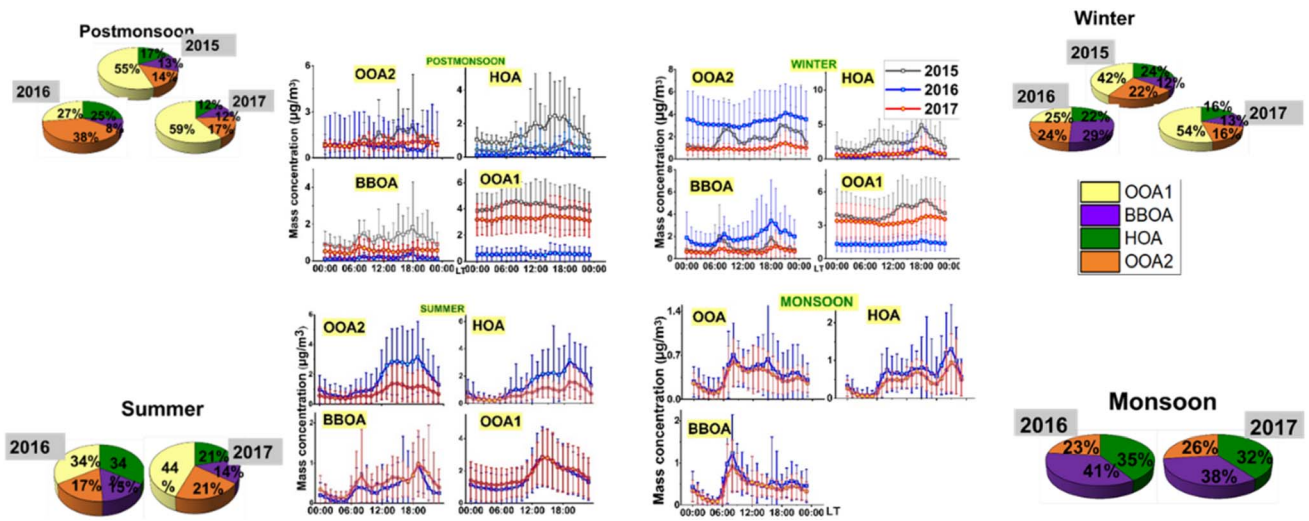

Fig. 7 Seasonally averaged diurnal variation of OA factors and percentage contribution of OA factors for 2015, 2016 and 2017.

oxygenated organic compounds under high relative humidity and low temperature. This diurnal pattern of OOA1 supports contributions from both local and regional transport. HOAs showed peaks at marker ions at m/z 41, 55 and 57, indicating that there might be some contribution from cooking activities also. HOA diurnal variation showed an afternoon peak (11:00–15:00 LT) related to cooking activities. As the profile of cooking OAs (COAs) is similar to that of HOAs, the ratio of m/z 55 : 57 (marker ions of COAs) was calculated. On the basis of a high m/z 55 : 57 ratio (1.3–1.6), the contribution by cooking activity to HOAs was confirmed. The evening peak of HOAs can be attributed to vehicular emissions. BBOAs showed morning and evening peaks, which may be due to anthropogenic activities like charcoal and wood burning. BBOAs and OOA1 showed similar diurnal patterns in 2016 and 2017, whereas OOA2 and HOAs exhibited higher concentrations in 2016.

The mass concentration of OA-factors during the monsoon season was lower than in summer. The monsoon season showed the highest contribution from BBOAs (38–41%) followed by HOAs (32–35%) and least from OOAs (23–26%). The higher contribution of primary organic aerosols (BBOAs and HOAs) than secondary organic aerosols showed the dominance of primary emission. The diurnal variation of HOAs showed a daytime build-up and a night-time (22:00 LT) peak due to vehicular emissions. Higher m/z 55 : 57 ratio (1.8–2) suggested contributions from COA emission to HOAs. On the other hand, BBOAs showed a morning (08:00 LT) peak and moderately high levels in the evening, which may be attributed to biofuel burning as suggested by the m/z 60 : 73 ratio (2.5–2.7).[69] OOAs showed high morning levels attributed by photochemical SOA formation declining with time. The lower OOA contribution to the OAs in the monsoon season in comparison to other seasons might be due to the washout of fresh and transported aerosols and low photochemical production in the presence of lower solar radiation. The percentage contribution of OA sources and the diurnal trend during 2016 and 2017 were comparable.

The source apportionment results have important implications for air quality management in the region. The significant contribution of BBOAs, particularly during the winter and monsoon seasons, highlights the need for stricter regulation of residential biomass burning and promotion of cleaner cooking and heating alternatives. The consistent presence of HOA across all seasons, with pronounced evening peaks, indicates the importance of controlling vehicular emissions through improved traffic management, stricter emission standards, and promotion of cleaner fuels and electric mobility.

The dominance of OOAs, especially during the post-monsoon and winter seasons, suggests that secondary organic aerosol formation plays a critical role in the OA burden. This underscores the need to control precursor emissions, such as volatile organic compounds (VOCs) and NO_x, from both anthropogenic and biogenic sources. Regional transport of aged aerosols further indicates that local mitigation strategies should be complemented by regional-scale air quality management policies.

Season-specific mitigation strategies, such as controlling biomass burning during winter and post-monsoon periods and reducing precursor emissions during high photochemical activity in summer, can significantly improve air quality in the region.

4 Conclusion

In the present study, high-resolution observations of NR-PM_1 chemical composition from a high-altitude site made over the course of October 2015 to February 2018 across all four seasons are reported. These measurements are important for a better understanding of background air quality in a remote site. The variation of aerosol species within seasons across different years is elaborated. The following conclusions can be drawn from the present study:

1. Organic aerosols (OAs) dominated the NR-PM_1 mass ($55 \pm 16\%$), highlighting their central role in submicron aerosol loading and indicating the importance of carbonaceous emissions in the region. The aerosol neutralization ratio (ANR) revealed predominantly neutralized particles, suggesting efficient interaction between acidic species and ammonia, particularly under conditions of low temperature and high relative humidity. The pronounced seasonal trend (winter > post-monsoon > summer > monsoon) reflects the combined influence of enhanced emissions, unfavourable dispersion conditions, and increased secondary aerosol formation during colder months. In contrast, lower concentrations during the monsoon season emphasize the role of wet scavenging and reduced photochemical activity.

2. Distinct diurnal patterns of NR-PM_1 species across seasons indicate the strong influence of boundary layer dynamics and source-specific emission timing (*e.g.*, traffic and residential activities), while the relatively small interannual variability suggests that seasonal meteorology exerts a stronger control on aerosol characteristics than year-to-year emission changes. These findings underscore the importance of targeting wintertime emissions and secondary aerosol precursors for effective air quality management, as well as the need to consider meteorology-driven variability in designing mitigation strategies.

3. As aerosol concentrations are also influenced by meteorological factors, variations in WS, RH, Temp, SR, accumulated rainfall and PBLH were also compared across all seasons in different years. In each season, SR, RH, Temp and WS were comparable in all the years, whereas PBLH and accumulated rainfall showed variation. The higher percentage of continental air masses arriving at the study site over the years indicated an increasing contribution from the continental landmass to aerosol concentrations at the study site.

4. The dominant fraction of NR-PM_1, OA was classified into different factors: HOA, BBOA, OOA1 and OOA2 to identify the source contributions. It was observed that more than half of OA comes from secondary emission sources during the post-monsoon, winter and summer seasons. The percentage contribution of OA factors showed variability across years within seasons.

A comparison of interannual variability indicates that while the overall seasonal trends in NR-PM_1 and its components remain consistent across the study period, the magnitude of concentrations and relative source contributions exhibit

notable year-to-year differences. For example, variations in the contribution of secondary organic aerosols (SOAs) and sulphates across different years suggest sensitivity to changes in meteorological conditions and precursor availability. This highlights a key advantage of multi-year observations over single-year campaigns. A one-year dataset may capture the general seasonal cycle; however, it may not adequately represent the full range of variability associated with changing meteorology, emission patterns, and regional transport. In contrast, a three-year dataset enables more robust characterization of aerosol processes by distinguishing persistent seasonal features from year-specific anomalies.

While the interpretations presented in this study are supported by observed temporal patterns and established atmospheric processes, uncertainties arise from both measurement limitations and source apportionment methods. The ACSM-derived mass concentrations are subject to uncertainties of ~20–30%, primarily associated with assumptions such as collection efficiency and ionization efficiency. In addition, PMF analysis introduces uncertainties related to factor selection, rotational ambiguity, and the lack of unique tracers for certain sources. As a result, the resolved OAs should be interpreted as representative source proxies rather than exact source contributions. Furthermore, some process-level interpretations (*e.g.*, photochemical production, biomass burning influence, and gas–particle partitioning) are based on consistency with known atmospheric behaviour rather than direct tracer-based confirmation and therefore carry inherent uncertainty. Despite this, the robustness of the results is supported by the consistency of seasonal patterns across multiple years and agreement with established literature. Importantly, the multi-year, high time-resolution dataset presented in this study has strong potential for predictive applications. Such long-term chemically resolved datasets can serve as valuable inputs for statistical and machine learning models aimed at forecasting air quality and understanding aerosol processes. By capturing seasonal cycles, inter-annual variability, and source-specific signatures, the dataset can help improve model training, reduce uncertainty in predictions, and enhance the representation of secondary aerosol formation pathways in data-driven frameworks.

Author contributions

Sonal Kumari – conceptualization, investigation, methodology, formal analysis, writing – original draft; G. Pandithurai – funding acquisition, project administration, resources, supervision, writing – review and editing; Pallavi Padwal – writing – review and editing; Rohit D. Patil – data curation; V. Anil Kumar – data curation; P.P. Leena – writing – review and editing; Sachin S. Patil – data curation; Ajit Waware – data curation; Lalit R. Chaudhari – data curation.

Conflicts of interest

The authors declare that they have no known competing financial interests or personal relationships that could have appeared to influence the work reported in this paper.

Data availability

Data will be provided on request to the project director.

Supplementary information (SI) is available. See DOI: https://doi.org/10.1039/d6ea00013d.

Acknowledgements

The Indian Institute of Tropical Meteorology (IITM) and High-Altitude Cloud Physics Laboratory (HACPL) are fully funded by Ministry of Earth Sciences, Govt of India. The authors are thankful to Director, IITM for encouragement. The authors acknowledge the HACPL team members for data collection.

References

1 J. H. Seinfeld and S. N. Pandis, *Atmospheric Chemistry and Physics: from Air Pollution to Climate Change*, Wiley, New Jersey, 2nd edn, 2006.
2 A. A. Presto, M. A. Miracolo, J. H. Kroll, D. R. Worsnop, A. L. Robinson and N. M. Donahue, Intermediate-volatility organic compounds: a potential source of ambient oxidized organic aerosol, *Environ. Sci. Technol.*, 2009, **43**, 4744–4749.
3 A. Tandon, S. Yadav and A. K. Attri, Coupling between meteorological factors and ambient aerosol load, *Atmos. Environ.*, 2010, **44**, 1237–1243.
4 M. Yang, C. Chu, M. S. Bloom, S. Li, G. Chen, J. Heinrich, I. Markevych, L. D. Knibbs, G. Bowatte, S. C. Dharmage and M. Komppula, Is smaller worse? New insights about associations of PM_1 and respiratory health in children and adolescents, *Environ. Int.*, 2018, **120**, 516–524.
5 J. L. Jimenez, M. R. Canagaratna, N. M. Donahue, A. S. H. Prevot, Q. Zhang, J. H. Kroll, P. F. DeCarlo, J. D. Allan, H. Coe, N. L. Ng and A. C. Aiken, Evolution of organic aerosols in the atmosphere, *Science*, 2009, **326**, 1525–1529.
6 J. H. Kroll and J. H. Seinfeld, Chemistry of secondary organic aerosol: formation and evolution of low-volatility organics in the atmosphere, *Atmos. Environ.*, 2008, **42**, 3593–3624.
7 J. P. Reid, A. K. Bertram, D. O. Topping, A. Laskin, S. T. Martin, M. D. Petters, F. D. Pope and G. Rovelli, The viscosity of atmospherically relevant organic particles, *Nat. Commun.*, 2018, **9**, 956.
8 P. K. Saha, A. Khlystov, K. Yahya, Y. Zhang, L. Xu, N. L. Ng and A. P. Grieshop, Quantifying the volatility of organic aerosol in the southeastern United States, *Atmos. Chem. Phys.*, 2017, **17**, 501–520.
9 R. Y. W. Chang, J. G. Slowik, N. C. Shantz, A. Vlasenko, J. Liggio, S. J. Sjostedt, W. R. Leaitch and J. P. D. Abbatt, The hygroscopicity parameter (κ) of ambient organic aerosol at a field site subject to biogenic and anthropogenic influences, *Atmos. Chem. Phys.*, 2010, **10**, 5047–5064.
10 J. T. Jayne, D. C. Leard, X. Zhang, P. Davidovits, K. A. Smith, C. E. Kolb and D. R. Worsnop, Development of an aerosol

mass spectrometer for size and composition analysis of submicron particles, *Aerosol Sci. Technol.*, 2000, **33**, 49–70.

11 N. L. Ng, S. C. Herndon, A. Trimborn, M. R. Canagaratna, P. L. Croteau, T. B. Onasch, D. Sueper, D. R. Worsnop, Q. Zhang, Y. L. Sun and J. T. Jayne, An aerosol chemical speciation monitor (ACSM) for routine monitoring of the composition and mass concentrations of ambient aerosol, *Aerosol Sci. Technol.*, 2011, **45**, 780–794.

12 R. Fröhlich, M. J. Cubison, J. G. Slowik, N. Bukowiecki, A. S. H. Prévôt, U. Baltensperger, J. Schneider, J. R. Kimmel, M. Gonin, U. Rohner, D. R. Worsnop and J. T. Jayne, The ToF-ACSM: a portable aerosol chemical speciation monitor with TOFMS detection, *Atmos. Meas. Tech.*, 2013, **6**, 3225–3241.

13 R. Fröhlich, M. J. Cubison, J. G. Slowik, N. Bukowiecki, F. Canonaco, P. L. Croteau, M. Gysel, S. Henne, E. Herrmann, J. T. Jayne, M. Steinbacher, D. R. Worsnop, U. Baltensperger and A. S. H. Prévôt, Fourteen months of online measurements of non-refractory submicron aerosol at the Jungfraujoch, *Atmos. Chem. Phys.*, 2015, **15**, 11373–11398.

14 M. Bressi, F. Cavalli, J. P. Putaud, R. Fröhlich, J.-E. Petit, W. Aas, M. Äijälä, A. Alastuey, J. D. Allan, M. Aurela, M. Berico, A. Bougiatioti, N. Bukowiecki, F. Canonaco, V. Crenn, S. Dusanter, M. Ehn, M. Elsasser, H. Flentje, P. Graf, D. C. Green, L. Heikkinen, H. Hermann, R. Holzinger, C. Hueglin, H. Keernik, A. Kiendler-Scharr, L. Kubelová, C. Lunder, M. Maasikmets, O. Makeš, A. Malaguti, N. Mihalopoulos, J. B. Nicolas, C. O'Dowd, J. Ovadnevaite, E. Petralia, L. Poulain, M. Priestman, V. Riffault, A. Ripoll, P. Schlag, J. Schwarz, J. Sciare, J. Slowik, Y. Sosedova, I. Stavroulas, E. Teinemaa, M. Via, P. Vodička, P. I. Williams, A. Wiedensohler, D. E. Young, S. Zhang, O. Favez, M. C. Minguillón and A. S. H. Prévôt, A European aerosol phenomenology – high-time-resolution chemical characteristics of submicron particulate matter, *Atmos. Environ. X*, 2021, **10**, 100108.

15 S. Chen, R. Zhang, R. Mao, Y. Zhang, Y. Chen, Z. Ji, Y. Gong and Y. Guan, Sources, characteristics and climate impact of light-absorbing aerosols over the Tibetan Plateau, *Earth-Sci. Rev.*, 2022, **232**, 104111.

16 C. O'Dowd, D. Ceburnis, J. Ovadnevaite, A. Vaishya, M. Rinaldi and M. C. Facchini, Do anthropogenic, continental or coastal aerosol sources impact on a marine aerosol signature at Mace Head?, *Atmos. Chem. Phys.*, 2014, **14**, 10687–10704.

17 V. Kumar, S. Giannoukos, S. L. Haslett, Y. Tong, A. Singh, A. Bertrand, C. P. Lee, D. S. Wang, D. Bhattu, G. Stefenelli, J. S. Dave, J. V. Puthussery, L. Qi, P. Vats, P. Rai, R. Casotto, R. Satish, S. Mishra, V. Pospisilova, C. Mohr, D. M. Bell, D. Ganguly, V. Verma, N. Rastogi, U. Baltensperger, S. N. Tripathi, A. S. H. Prévôt and J. G. Slowik, Highly time-resolved chemical speciation and source apportionment of organic aerosol components in Delhi, *Atmos. Chem. Phys.*, 2022, **22**, 7739–7761.

18 L. L. Tang, H. X. Yu, A. J. Ding, Y. J. Zhang, W. Qin, Z. Wang, W. T. Chen, Y. Hua and X. X. Yang, Regional contribution to PM_1 pollution during winter haze in the Yangtze River Delta, *Sci. Total Environ.*, 2016, **541**, 161–166.

19 P. Pokorná, N. Zíková, P. Vodička, R. Lhotka, S. Mbengue, A. Holubová Šmejkalová, V. Riffault, J. Ondráček, J. Schwarz and V. Ždímal, Chemically speciated mass size distribution and origin of non-refractory PM_1, *Atmos. Chem. Phys.*, 2022, **22**, 5829–5858.

20 H. Zhong, R.-J. Huang, C. Lin, W. Xu, J. Duan, Y. Gu, W. Huang, H. Ni, C. Zhu, Y. You, Y. Wu, R. Zhang, J. Ovadnevaite, D. Ceburnis and C. D. O'Dowd, On the contribution of long-distance transport to secondary aerosol formation and aging, *Atmos. Chem. Phys.*, 2022, **22**, 9513–9524.

21 M. Hallquist, J. C. Wenger, U. Baltensperger, Y. Rudich, D. Simpson, M. Claeys, J. Dommen, N. M. Donahue, C. George, A. H. Goldstein, J. F. Hamilton, H. Herrmann, T. Hoffmann, Y. Iinuma, M. Jang, M. E. Jenkin, J. L. Jimenez, A. Kiendler-Scharr, W. Maenhaut, G. McFiggans, Th. F. Mentel, A. Monod, A. S. H. Prévôt, J. H. Seinfeld, J. D. Surratt, R. Szmigielski and J. Wildt, The formation, properties and impact of secondary organic aerosol: current and emerging issues, *Atmos. Chem. Phys.*, 2009, **9**, 5155–5236.

22 A. I. Calvo, C. Alves, A. Castro, V. Pont, A. M. Vicente and R. Fraile, Research on aerosol sources and chemical composition: past, current and emerging issues, *Atmos. Res.*, 2013, **120–121**, 1–28.

23 J. Haywood and O. Boucher, Estimates of the direct and indirect radiative forcing due to tropospheric aerosols: a review, *Rev. Geophys.*, 2000, **38**, 513–543.

24 H. Timonen, J. L. Ambrose and D. A. Jaffe, Oxidation of elemental Hg in anthropogenic and marine air masses, *Atmos. Chem. Phys.*, 2013, **13**, 2827–2836.

25 G. Chen, F. Canonaco, J. G. Slowik, K. R. Daellenbach, A. Tobler, J. E. Petit, O. Favez, I. Stavroulas, N. Mihalopoulos, E. Gerasopoulos and I. El Haddad, Real-time source apportionment of organic aerosols in three European cities, *Environ. Sci. Technol.*, 2022, **56**, 15290–15297.

26 P. Acharja, A. Vispute, P. Lonkar, S. W. Gosavi, S. Debnath, N. G. Dhangar, K. Ali, G. Govardhan and S. D. Ghude, Size-resolved compositional analysis and source apportionment of submicron aerosol during lockdown period using HR-ToF-AMS, *Aerosol Air Qual. Res.*, 2022, **22**, 220108.

27 T. C. Ajith, S. K. Kompalli, V. S. Nair and S. S. Babu, Mesoscale variations of the chemical composition of submicron aerosols and its influence on cloud condensation nuclei activation, *Atmos. Environ.*, 2022, **268**, 118778.

28 T. C. Ajith, S. K. Kompalli, J. Allan, H. Coe and S. S. Babu, Formation pathways of organic aerosols over a tropical coastal atmosphere, *Atmos. Environ.*, 2023, **309**, 119881.

29 S. Bhandari, S. Gani, K. Patel, D. S. Wang, P. Soni, Z. Arub, G. Habib, J. S. Apte and L. Hildebrandt Ruiz, Sources and atmospheric dynamics of organic aerosol in New Delhi, India: insights from receptor modeling, *Atmos. Chem. Phys.*, 2020, **20**, 735–752.

30 S. Bhandari, Z. Arub, G. Habib, J. S. Apte and L. Hildebrandt Ruiz, Contributions of primary sources to submicron organic aerosols in Delhi, India, *Atmos. Chem. Phys.*, 2022, **22**, 13631–13657.

31 J. M. Cash, B. Langford, C. Di Marco, N. Mullinger, J. Allan, E. Reyes-Villegas, R. Joshi, M. R. Heal, W. J. F. Acton, N. Hewitt and P. Misztal, Seasonal analysis of submicron aerosol in Old Delhi using high-resolution aerosol mass spectrometry: chemical characterisation, source apportionment and new marker identification, *Atmos. Chem. Phys.*, 2021, **21**, 10133–10158.

32 A. Chakraborty, A. K. Mandariya, R. Chakraborti, T. Gupta and S. N. Tripathi, Realtime chemical characterization of post-monsoon organic aerosols in a polluted urban city: sources, composition and seasonal comparison, *Environ. Pollut.*, 2018, **232**, 310–321.

33 J. Dave, R. Meena, A. Singh and N. Rastogi, Effect of COVID-19 lockdown on the concentration and composition of NR-PM2.5 over Ahmedabad, western India, *Urban Clim.*, 2021, **37**, 100818.

34 S. Gani, S. Bhandari, S. Seraj, D. S. Wang, K. Patel, P. Soni, Z. Arub, G. Habib, L. Hildebrandt Ruiz and J. S. Apte, Submicron aerosol composition in the world's most polluted megacity: the Delhi Aerosol Supersite study, *Atmos. Chem. Phys.*, 2019, **19**, 6843–6859.

35 S. S. Gunthe, P. Liu, U. Panda, S. S. Raj, A. Sharma, E. Darbyshire, E. Reyes-Villegas, J. Allan, Y. Chen, X. Wang and S. Song, Enhanced aerosol particle growth sustained by high continental chlorine emission in India, *Nat. Geosci.*, 2021, **14**, 77–84.

36 S. M. Kommula, P. Upasana, A. Sharma, S. S. Raj, E. Reyes-Villegas, T. Liu, J. D. Allan, C. Jose, M. L. Pöhlker, R. Ravikrishna and P. Liu, Chemical characterization and source apportionment of organic aerosols in the coastal city of Chennai, India, *ACS Earth Space Chem.*, 2021, **5**, 3197–3209.

37 S. K. Kompalli, S. N. Suresh Babu, S. K. Satheesh, K. Krishna Moorthy, T. Das, R. Boopathy, D. Liu, E. Darbyshire, J. D. Allan, J. Brooks and M. J. Flynn, Seasonal contrast in size distributions and mixing state of black carbon and its association with PM1 chemical composition from the eastern coast of India, *Atmos. Chem. Phys.*, 2020, **20**, 3965–3985.

38 S. K. Kompalli, S. N. S. Babu, K. K. Moorthy, S. K. Satheesh, M. M. Gogoi, V. S. Nair, V. N. Jayachandran, D. Liu, M. J. Flynn and H. Coe, Mixing state of refractory black carbon aerosol in the South Asian outflow over the northern Indian Ocean during winter, *Atmos. Chem. Phys.*, 2021, **21**, 9173–9199.

39 V. Lalchandani, V. Kumar, A. Tobler, N. M. Thamban, S. Mishra, J. G. Slowik, D. Bhattu, P. Rai, R. Satish, D. Ganguly and S. Tiwari, Real-time characterization and source apportionment of fine particulate matter in the Delhi megacity during late winter, *Sci. Total Environ.*, 2021, **770**, 145324.

40 S. Mukherjee, V. Singla, G. Pandithurai, P. D. Safai, G. S. Meena, K. K. Dani and V. A. Kumar, Seasonal variability in chemical composition and source apportionment of submicron aerosol over a high-altitude site in the Western Ghats, India, *Atmos. Environ.*, 2018, **180**, 79–92.

41 K. Patel, S. Bhandari, S. Gani, M. J. Campmier, P. Kumar, G. Habib, J. S. Apte and L. Hildebrandt Ruiz, Sources and dynamics of submicron aerosol during the autumn onset of the air pollution season in Delhi, India, *ACS Earth Space Chem.*, 2021, **5**, 118–128.

42 A. Singh, R. V. Satish and N. Rastogi, Characteristics and sources of fine organic aerosol over a semi-arid urban city of western India using HR-ToF-AMS, *Atmos. Environ.*, 2019, **208**, 103–112.

43 N. M. Thamban, B. Joshi, S. N. Tripathi, D. Sueper, M. R. Canagaratna, S. P. Moosakutty, R. Satish and N. Rastogi, Evolution of aerosol size and composition in the Indo-Gangetic Plain: size-resolved analysis of high-resolution aerosol mass spectra, *ACS Earth Space Chem.*, 2019, **3**, 823–832.

44 A. S. Vispute, P. Acharja, S. W. Gosavi, G. Govardhan, V. Ruge, M. N. Patil, T. Dharmaraj and S. D. Ghude, Source characteristics of non-refractory particulate matter (NR-PM1) using HR-ToF-AMS measurements in an urban industrial city in India, *Atmos. Environ.*, 2025, 121186.

45 Census Commission of India, *Census of India 2011: Provisional Population Totals*, Government of India, 2011.

46 V. Singla, S. Mukherjee, G. Pandithurai, K. K. Dani and P. D. Safai, Evidence of organonitrate formation at a high-altitude site, Mahabaleshwar, during the pre-monsoon season, *Aerosol Air Qual. Res.*, 2017, **19**, 1241–1251.

47 P. S. Liu, R. Deng, K. A. Smith, L. R. Williams, J. T. Jayne, M. R. Canagaratna, K. Moore, T. B. Onasch, D. R. Worsnop and T. Deshler, Transmission efficiency of an aerodynamic focusing lens system for the aerosol mass spectrometer, *Aerosol Sci. Technol.*, 2007, **41**, 721–733.

48 P. Paatero and U. Tapper, Positive matrix factorization: a non-negative factor model with optimal utilization of error estimates of data values, *Environmetrics*, 1994, **5**, 111–126.

49 J. Xu, Q. Zhang, M. Chen, X. Ge, J. Ren and D. Qin, Chemical composition, sources and processes of urban aerosols during summertime in northwest China, *Atmos. Chem. Phys.*, 2014, **14**, 12593–12611.

50 D. C. S. Beddows, R. M. Harrison, D. C. Green and G. W. Fuller, Receptor modelling of particle composition and size distribution at a background site in London, *Atmos. Chem. Phys.*, 2015, **15**, 10107–10125.

51 Y. Sun, C. Chen, Y. Zhang, W. Xu, L. Zhou, X. Cheng, H. Zheng, D. Ji, J. Li, X. Tang, P. Fu and Z. Wang, Rapid formation and evolution of an extreme haze episode in northern China during winter 2015, *Sci. Rep.*, 2016, **6**, 27151.

52 Q. Zhang, J. L. Jimenez, M. R. Canagaratna, I. M. Ulbrich, N. L. Ng, D. R. Worsnop and Y. Sun, Understanding atmospheric organic aerosols *via* factor analysis of aerosol mass spectrometry, *Anal. Bioanal. Chem.*, 2011, **401**, 3045–3067.

53 I. M. Ulbrich, M. R. Canagaratna, Q. Zhang, D. R. Worsnop and J. L. Jimenez, Interpretation of organic components from positive matrix factorization of aerosol mass spectrometric data, *Atmos. Chem. Phys.*, 2009, **9**, 2891–2918.
54 Q. Zhang, J. L. Jimenez, M. R. Canagaratna, J. D. Allan, H. Coe, I. Ulbrich, M. R. Alfarra, A. Takami, A. M. Middlebrook, Y. L. Sun, K. Dzepina, E. Dunlea, K. Docherty, P. F. DeCarlo, D. Salcedo, T. Onasch, J. T. Jayne, T. Miyoshi, A. Shimono, S. Hatakeyama, N. Takegawa, Y. Kondo, J. Schneider, F. Drewnick, S. Borrmann, S. Weimer, K. Demerjian, P. Williams, K. Bower, R. Bahreini, L. Cottrell, R. J. Griffin, J. Rautiainen, J. Y. Sun, Y. M. Zhang and D. R. Worsnop, Ubiquity and dominance of oxygenated species in organic aerosols in anthropogenically influenced Northern Hemisphere midlatitudes, *Geophys. Res. Lett.*, 2007, **34**, L13801.
55 A. Chakraborty, D. Bhattu, T. Gupta, S. N. Tripathi and M. R. Canagaratna, Real-time measurements of ambient aerosols in a polluted Indian city during foggy and non-foggy periods, *J. Geophys. Res. Atmos.*, 2015, **120**, 9006–9019.
56 D. M. Chate, P. S. P. Rao, M. S. Naik, G. A. Momin, P. D. Safai and K. Ali, Scavenging of aerosols and their chemical species by rain, *Atmos. Environ.*, 2003, **37**, 2477–2484.
57 B. Sharma, S. Jia, A. J. Polana, M. S. Ahmed, R. R. Haque, S. Singh, J. Mao and S. Sarkar, Seasonal variations in aerosol acidity and its driving factors in the eastern Indo-Gangetic Plain, *Chemosphere*, 2022, **305**, 135490.
58 N. Tripathi and L. K. Sahu, Enhancement of biogenic VOC emissions in a semi-arid region of India during the winter–summer transition, *Atmos. Chem. Phys.*, 2020, **20**, 13011–13027.
59 Y. Qiu, Z. Wu, R. Man, T. Zong, Y. Liu, X. Meng, J. Chen, S. Chen, S. Yang, B. Yuan and M. Song, Secondary aerosol formation drives particulate matter pollution over megacities in East Asia, *Atmos. Environ.*, 2023, **301**, 119702.
60 W. Hu, M. Hu, W.-W. Hu, J. Zheng, C. Chen, Y. Wu and S. Guo, Seasonal variations in high-time-resolution chemical composition and sources of submicron aerosols in Beijing, *Atmos. Chem. Phys.*, 2017, **17**, 9979–10000.
61 Y. Sun, Z. Wang, H. Dong, T. Yang, J. Li, X. Pan, P. Chen and J. T. Jayne, Characterization of summer organic and inorganic aerosols in Beijing using an aerosol chemical speciation monitor, *Atmos. Environ.*, 2012, **51**, 250–259.
62 S. Guo, M. Hu, Z. B. Wang, J. Slanina and Y. L. Zhao, Size-resolved aerosol water-soluble ionic composition in summer Beijing, *Atmos. Chem. Phys.*, 2010, **10**, 947–959.
63 R. Huang, J. Duan, Y. Li, Q. Chen, Y. Chen, M. Tang, L. Yang, H. Ni, C. Lin, W. Xu, Y. Liu, C. Chen, Z. Yan, J. Ovadnevaite, D. Ceburnis, U. Dusek, J. Cao, T. Hoffmann and C. D. O'Dowd, Effects of ammonia and alkaline metals on particulate sulphate and nitrate formation in wintertime Beijing, *Sci. Total Environ.*, 2020, **717**, 137190.
64 P. S. Buchunde, P. D. Safai, S. Mukherjee, M. P. Raju, G. S. Meena, S. M. Sonbawne, K. K. Dani and G. Pandithurai, Seasonal abundances of primary and secondary carbonaceous aerosols at a high-altitude site in the Western Ghats, India, *Air Qual. Atmos. Health*, 2021, **14**, 1–12.
65 M. R. Canagaratna, J. T. Jayne, D. A. Ghertner, S. Herndon, Q. Shi, J. L. Jimenez, P. J. Silva, P. Williams, T. Lanni, F. Drewnick and K. L. Demerjian, Chase studies of particulate emissions from in-use New York City vehicles, *Aerosol Sci. Technol.*, 2004, **38**, 555–573.
66 A. C. Aiken, D. Salcedo, M. J. Cubison, J. A. Huffman, P. F. DeCarlo, I. M. Ulbrich, K. S. Docherty, D. Sueper, J. R. Kimmel, D. R. Worsnop and A. Trimborn, Mexico City aerosol analysis during MILAGRO using high-resolution aerosol mass spectrometry, *Atmos. Chem. Phys.*, 2009, **9**, 6633–6653.
67 M. R. Alfarra, A. S. H. Prévôt, S. Szidat, J. Sandradewi, S. Weimer, V. A. Lanz, D. Schreiber, M. Mohr and U. Baltensperger, Identification of the mass spectral signature of organic aerosols from wood burning emissions, *Environ. Sci. Technol.*, 2007, **41**, 5770–5777.
68 C. Mohr, P. F. DeCarlo, M. F. Heringa, R. Chirico, J. G. Slowik, R. Richter, C. Reche, A. Alastuey, X. Querol, R. Seco and J. Peñuelas, Identification and quantification of organic aerosol from cooking and other sources in Barcelona, *Atmos. Chem. Phys.*, 2012, **12**, 1649–1665.
69 M. J. Cubison, A. M. Ortega, P. L. Hayes, D. K. Farmer, D. Day, M. J. Lechner, W. H. Brune, E. Apel, G. S. Diskin, J. A. Fisher, H. E. Fuelberg, A. Hecobian, D. J. Knapp, T. Mikoviny, D. Riemer, G. W. Sachse, W. Sessions, R. J. Weber, A. J. Weinheimer, A. Wisthaler and J. L. Jimenez, Effects of aging on organic aerosol from open biomass burning smoke, *Atmos. Chem. Phys.*, 2011, **11**, 12049–12064.

